Ethanol Conversion to Propylene over Zn/Hβ Catalysts: Influence of Zinc Precursors

Ting Bai , Xiaohui Li , Liang Ding , Jin Wang , Yong-Shan Xiao * , Bin Cao *

Posted Date: 22 March 2024

doi: 10.20944/preprints202403.1382.v1

Keywords: ethanol; propylene; zinc; Hβ; acidity; coke deposition

Article

Ethanol Conversion to Propylene over Zn/Hβ Catalysts: Influence of Zinc Precursors

Ting Bai [1], Xiaohui Li [1], Liang Ding [1], Jin Wang [1], Yong-Shan Xiao [2,*] and Bin Cao [1,*]

[1] College of Chemistry and Chemical Engineering, Xi'an Shiyou University, Xi'an 710065, Shaanxi, China
[2] School of Chemistry & Chemical Engineering, Shaanxi Normal University, Xi'an 710119, China
* Correspondence: No. 18, East Dianzier Road, College of Chemistry and Chemical Engineering, Xi'an Shiyou University, Xi'an 710065, China. E-mail: caobinxys@126.com; No. 620, West Chang'an Avenue, School of Chemistry & Chemical Engineering, Shaanxi Normal University, Xi'an 710119, China, E-mail: xiaoys@snnu.edu.cn

Abstract: A series of Zn-modified Hβ (Zn/Hβ) catalysts were prepared by using the different zinc precursors such as $ZnSO_4{\cdot}7H_2O$, $ZnCl_2$, $C_4H_6O_4Zn{\cdot}2H_2O$ and $Zn(NO_3)_2{\cdot}6H_2O$, and their catalytic performance in the ethanol conversion to propylene reaction was evaluated. Results indicate the amount and strength distribution of acid sites of the Zn/Hβ catalysts were easily tuned by employing different type of zinc precursors. More importantly, when the zinc species were introduced to the Hβ, the propylene yield was significantly enhanced, whereas the yields of the byproducts such as ethylene and C_2-C_4 alkanes were remarkably suppressed. For the catalyst prepared by using the $ZnCl_2$ precursor (Zn/Hβ-C), a higher propylene yield up to 43.4% was achieved as a result of the moderate amount and strength distribution of acid sites. The average coking rate of the used Zn/Hβ catalysts strongly depended on the amount of total acid sites, especially the strong acid sites, i.e., the higher the amount of total acid sites of the catalyst, the greater the average coking rate. For the catalyst prepared by using the $ZnSO_4{\cdot}7H_2O$ precursor, Zn/Hβ-S exhibited a better stability even after depositing more coke, which is due to the higher amount of strong acid sites.

Keywords: ethanol; propylene; zinc; Hβ, acidity; coke deposition

1. Introduction

Propylene is widely used in the production of highly valuable chemicals such as polypropylene, acrylonitrile, propylene oxide, acetone and so on [1–3]. Propylene is mainly produced as co-product from naphtha steam cracking and catalytic cracking, which are strongly dependent on fossil fuels [4]. In addition, methanol to propylene (MTP) and propane dehydrogenation (PDH) process have been developed by using nonpetroleum resources [5,6]. Nevertheless, the production of propylene is still in short supply owing to the increasing demand for its derivatives. With the shortage of fossil fuels and environmental protection, the conversion of bio-ethanol to propylene has attracted much attention in the last years since bioethanol production technology get rapid developed. The ethanol to propylene reaction (ETP) is considered to be a carbon-neutral process, which can reduce the damage to environment and relieve the pressure of oil shortage [7–9].

To date, the catalysts for the ETP reaction are mainly concentrated on zeolites and transition metal oxides. For the acidic zeolites such as HZSM-5, ethanol is firstly dehydrated to ethylene on the acid sites, followed by the oligomerization-cracking reactions to form propylene as a result of the shape selectivity [10–14]. However, the randomness of the oligomerization reaction results in the propylene selectivity as low as around 20-30%. Meanwhile, the side reactions such as aromatization, cyclization and hydrogen transfer easily occur on the strong acid sites, giving rise to the extensive coke deposition and fast deactivation of catalyst [9,15]. Recently, substantial attention have been paid on the transition metal oxides for the ETP reaction [16–20]. Iwamoto et al. [17,18] found that a 30%

 doi:10.20944/preprints202403.1382.v1

yield of propylene was achieved over Y/CeO_2 in the presence of water, and a similar propylene yield of 34% was observed on Sc/In_2O_3 [21]. Xia et al. [20] reported that a 44% yield of propylene was achieved over Y/ZrO_2. The stability of metal oxides in the ETP reaction is significantly improved because of the fewer coke deposition than zeolites. However, a large amount of ethylene as high as 20-32% was also produced as the main byproduct as a result of the weak acid sites and the absence of the shape selectivity of pore window [18,21]. Thus, it is still a great challenge for developing the catalyst with a higher propylene selectivity and a better stability.

More recently, the metal oxide-zeolite composites for the ETP reaction are proposed for combining the merits of zeolite and metal oxide [22–25], which has been demonstrated to be an effective strategy for improving the propylene selectivity and stability of the catalyst. Typically, a relatively high propylene yield over the In_2O_3-beta composite can be kept stable at about 50% for 46 h under reaction condition of 460 °C and a space velocity of 0.2 h^{-1} [22]. Unfortunately, the expensive In_2O_3 precursor may limit its large-scaled preparation for industrial application. In this aspect, with optimizing the Si/Al ratio of HBeta zeolite and its ratio to $ZnCeO_x$, the composite of $ZnCeO_x$ and HBeta zeolite exhibits a higher propylene yield of more than 55% and an ethylene yield as low as 3% under the optimal reaction conditions, and the propylene yield remains stable at around 50% after three generation cycles [23]. These significant results can provide well understandings for a rational and controllable design of the metal oxide-zeolite composites with a higher propylene selectivity and a better stability. As is well known, the metal oxide precursors play a crucial role for the preparation of the metal oxide catalyst [26,27]. However, to the best of our knowledge, the effect of the metal oxide precursors for the hybrid catalysts in the ETP reaction has not been systematically investigated. There is still a lack of clear and well understanding on the effect of the metal oxide precursors. To this end, it is necessary to investigate the influence of metal oxide precursor on the metal oxide-zeolite composites in the ETP reaction.

In this work, a series of the Zn/Hβ catalysts have been prepared by using different zinc precursors such as $ZnSO_4{\cdot}7H_2O$, $ZnCl_2$, $C_4H_6O_4Zn{\cdot}2H_2O$, and $Zn(NO_3)_2{\cdot}6H_2O$. The physicochemical properties of the fresh and used catalysts were characterized by X-ray diffraction (XRD), temperature programmed desorption of ammonia (NH_3-TPD), N_2 adsorption-desorption, fourier transform infrared spectroscopy (FT-IR) and temperature programmed oxidation (TPO). The catalytic performance of Zn/Hβ catalysts in the ETP reaction was investigated. Based on the obtained results, the influence of zinc precursors on the acidic properties, catalytic performance and coke deposition of Zn/Hβ catalysts were rigorously elucidated.

2. Experimental

2.1. Chemicals

All chemicals with analytical grade were directly employed as received without further purifications. Zinc sulfate ($ZnSO_4{\cdot}7H_2O$), zinc chloride ($ZnCl_2$), zinc acetate ($C_4H_6O_4Zn{\cdot}2H_2O$) and zinc nitrate ($Zn(NO_3)_2{\cdot}6H_2O$) were purchased from *Shanghai Aladdin Biochemical Technology Co. Ltd.*, China. The Hβ zeolite (Si/Al = 100) was purchased from Tianjin Nanhua Catalyst Co. Ltd., China.

2.2. Catalyst preparation

A series of Zn/Hβ catalysts with 16 wt.% loading of zinc were prepared by wetness impregnation method. Typically, a desired amount of zinc precursor was dissolved in 50 mL of deionized water. The Hβ zeolite power was impregnated in the aqueous solution of different zinc precursors at 50 °C for 3 h. The impregnated power was dried at 110 °C for 12 h and then calcined at 450 °C for 4 h in air. The resulting Zn/Hβ catalysts were denoted as Zn/Hβ-S, Zn/Hβ-C, Zn/Hβ-Ac and Zn/Hβ-N, when $ZnSO_4{\cdot}7H_2O$, $ZnCl_2$, $C_4H_6O_4Zn{\cdot}2H_2O$ and $Zn(NO_3)_2{\cdot}6H_2O$ were used as the zinc precursor, respectively.

 doi:10.20944/preprints202403.1382.v1

2.3. Catalyst characterization

Powder X-ray diffraction (XRD) patterns of the samples were conducted on Rogaku Rotflex D/Max-C X-ray diffractometer with Cu Kα radiation (λ = 0.15046 nm) at 40 kV and 30 mA. N_2 adsorption-desorption characterization was performed on Micromeritics ASAP400 instrument at −196 °C. Prior to the adsorption, all the samples were pretreated under vacuum condition at 300 °C for 6 h. The specific surface area was calculated according to BET method. The micropore volume was obtained by *t*-plot analysis of the adsorption isotherm. The mesopore volume was obtained by BJH method. The ammonia temperature-programmed desorption (NH_3-TPD) and temperature-programmed oxidation (TPO) experiments were carried out on a continuous flow fixed-bed reactor system with thermal conductivity detector (TCD, Beifen Ruili GC-3400). For NH_3-TPD, the sample was pretreated in a N_2 flow at 200 °C for 2 h, and then cooled down to 50 °C. The NH_3 was injected to the sample until adsorption saturation. The sample was purged in a N_2 flow to remove the physically adsorbed NH_3 from the sample surface. NH_3-TPD was carried out from 50 to 600 °C with a heating rate of 10 °C min^{-1} in a N_2 flow. TPO was performed in an air flow from 50 to 800 °C with a heating rate of 10 °C/min. FTIR spectra of the samples were recorded by Nicolet FTIR 6700 spectrometer with resolution of 4 cm^{-1}.

2.4. Catalytic evaluation

The catalytic conversion of ethanol to propylene was carried out in a continuous-flow fixed-bed reactor. Prior to the evaluation, 0.5 g of catalyst (20-40 mesh) was pretreated in a N_2 flow at 400 °C for 30 min. The catalyst bed temperature was monitored by a K-type thermocouple in the catalyst bed. Ethanol was fed by a micro pump and vaporized. Ethanol and N_2 were mixed well and introduced into the reactor. The catalysts were evaluated under the reaction conditions of T = 500 °C, P = 0.1 MPa, P_{C2H5OH} = 0.02 MPa, and $WHSV$ = 2.8 h^{-1}. The outlet gas was analyzed by gas chromatography (GC-2060, Shanghai Ruimin Instrument Co. Ltd.) with two analytical modules. The products were separated by a KB-Al_2O_3/Na_2SO_4 capillary column and detected by a flame ionization detector (FID). Ethanol was identified by a GDX-103 packed column and detected by a thermal conductivity detector (TCD). After the reaction, the used catalyst bed was swept with a N_2 flow (40 cm^3/min) for 30 min in order to stabilize and homogenize the coke deposited on used catalysts for further analysis. The ethanol conversion and the yield of products were calculated on carbon basis.

3. Results

3.1. Structural and textural properties

The XRD patterns of the Hβ and Zn/Hβ catalysts are shown in Figure 1. A series of prominent diffraction peaks at 2θ of 7.8, 12.0, 13.6, 21.0, 22.4, 29.4, and 41.0° were observed for the Hβ and Zn/Hβ catalysts, which are typical characteristics of BEA structure of zeolite [24]. Compared with the parent Hβ, the peaks of the BEA structure of the Zn/Hβ were lower in different degrees, suggesting the crystallinity of Zn/Hβ catalysts is lower than Hβ. It is attributed to the collapse of the crystal structure during the impregnation and subsequent secondary calcination processes, and/or the coverage of zinc species on Hβ [28]. Moreover, a series of high diffraction peaks at 18.5, 26.2, 26.9, 29.2, 34.9, 35.6, 38.5, and 41.0° assigned to the $ZnSO_4$ were observed for Zn/Hβ-S, indicating the presence of a significant quantity of $ZnSO_4$ on the surface of Zn/Hβ-S [29]. Since the decomposition temperature of $ZnSO_4$ is significantly higher than 550 °C, most of the $ZnSO_4$ on the Zn/Hβ-S is well retained after calcination at 450 °C for 4 h [30]. In contrast, the diffraction peaks at 31.7, 34.4, 36.2, and 47.5° corresponding to the (100), (002), (101), and (102) lattice planes of ZnO were obviously detected on both Zn/Hβ-Ac and Zn/Hβ-N, suggesting the presence of large-sized and well-crystallized ZnO [31]. There were no diffraction peaks assigned to the detectable zinc species for Zn/Hβ-C, indicating the existence of highly dispersed zinc species.

 doi:10.20944/preprints202403.1382.v1

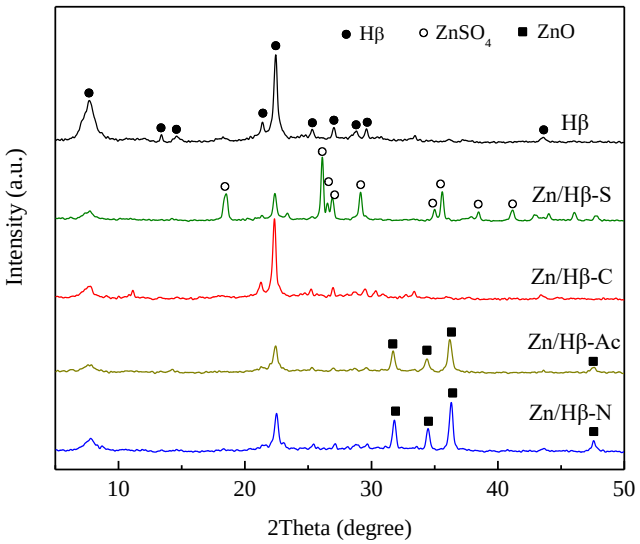

Figure 1. XRD patterns of the Hβ and Zn/Hβ catalysts.

Table 1 shows the textural properties of Hβ and Zn/Hβ catalysts. The BET specific surface area (S_{BET}) and total pore volume (V_{total}) of Hβ were 560.6 m^2/g and 0.36 cm^3/g, respectively. In contrast, Zn/Hβ catalysts showed much lower S_{BET} and V_{total}, i.e., 162.0~277.2 m^2/g for S_{BET}, and 0.13~0.27 cm^3/g for V_{total}. More importantly, a significant decline in the micropore volume (V_{micro}) was observed for all of the Zn/Hβ catalysts in comparison with Hβ, while very similar mesopore volume (V_{meso}) was obtained expect Zn/Hβ-S and Zn/Hβ-Ac. The V_{meso} of 0.17 cm^3/g for Zn/Hβ-Ac was higher than that of Hβ (0.13 cm^3/g) as a result of the structure defects or the appearance of intercrystalline pores, whereas the V_{meso} of Zn/Hβ-S was almost half that of Hβ. Considering the microporous structure of Hβ, it is well accepted that the high S_{BET} of Hβ was mainly contributed by the micropores. For this reason, the remarkable decrease in both the V_{total} and S_{BET} of Zn/Hβ catalysts was rigorously attributed to the decrease in the V_{micro} as a result of the partial pore blockage by the zinc species and/or collapse of pore channels.

Table 1. The textural properties of the Hβ and Zn/Hβ catalysts.

Catalysts	S_{BET} (m^2/g)	V_{micro} (cm^3/g)	V_{meso} (cm^3/g)	V_{total} (cm^3/g)
Hβ	560.6	0.23	0.13	0.36
Zn/Hβ-S	162.0	0.06	0.07	0.13
Zn/Hβ-C	216.7	0.09	0.11	0.20
Zn/Hβ-Ac	248.3	0.10	0.17	0.27
Zn/Hβ-N	277.2	0.12	0.12	0.24

3.2. Acidic properties

To reveal the acidic properties of the Hβ and Zn/Hβ catalysts, the NH_3-TPD experiments were conducted, and the results are shown in Figure 2. Generally, a broad NH_3 desorption peak was observed for all of the catalysts, indicating the presence of acid sites with varied strength. In this

 doi:10.20944/preprints202403.1382.v1

respect, the temperature at the peak maximum of NH_3 desorption is used as a common descriptor for determining the strength of acid sites. The peak temperature of weaker acid site is lower, and vice versa. To semi-quantify the varied strengths of acid sites, the broad NH_3 desorption peak was deconvoluted into three desorption peaks based on the peak temperature [10], as shown in Figure 2. The first desorption peak between 127 and 155 °C is ascribed to the weak acid sites. The second desorption peak between 183 and 260 °C is attributed to the medium acid sites. The final desorption peak at around 356-430 °C is associated to the strong acid sites. Although Zn/Hβ-S appeared two clear desorption peaks, the same procedure was practiced for a comparison purpose. Thus, the corresponding peak area of the NH_3 desorption is summarized in Table 2.

Apparently, the total amount of acid sites was decreased in the order of Zn/Hβ-S > Zn/Hβ-C > Hβ > Zn/Hβ-Ac > Zn/Hβ-N. Herein, the highest total amount of acid sites was achieved for Zn/Hβ-S, which was significantly dominated by the amount of strong acid sites. When the amount of strong acid sites was concerned, similar order of Zn/Hβ-S > Zn/Hβ-C > Hβ > Zn/Hβ-N ≈ Zn/Hβ-Ac was obtained. Moreover, the amounts of the weak, medium, and strong acid sites were almost the same in the case of Zn/Hβ-Ac. At the same time, the amounts of the weak and strong acid sites were very similar in the case of Hβ, slightly higher than that of the medium acid sites. For Zn/Hβ-C, the amount of medium acid sites was slightly lower than the strong acid sites, and much higher than the weak acid sites.

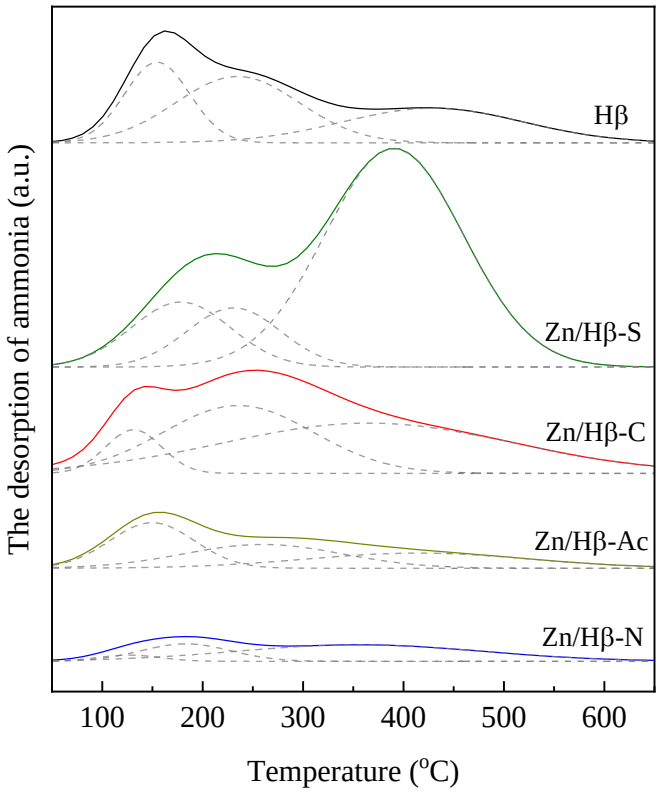

Figure 2. NH_3-TPD profiles of Hβ and Zn/Hβ catalysts.

Table 2. The amount and strength distribution of acid sites on Hβ and Zn/Hβ catalysts.

Catalysts	The amount of acid sites (a.u./g)			
	Weak (50-200 °C)	Medium (200-350 °C)	Strong (> 350 °C)	Total

 doi:10.20944/preprints202403.1382.v1

Hβ	71.8	111.7	85.1	268.6
Zn/Hβ-S	88.2	75.7	413.4	577.3
Zn/Hβ-C	33.4	139.3	199.9	372.6
Zn/Hβ-Ac	52.6	51.5	46.6	150.7
Zn/Hβ-N	5.3	21.4	55.8	82.5

3.3. Catalytic performance

All of the catalysts gave 100% ethanol conversion under the reaction conditions of T = 500 °C, P = 0.1 MPa, P_{C2H5OH} = 0.02 MPa, $WHSV$ = 2.8 h^{-1} and TOS = 1 h. However, the product distribution is significantly dependent on the composition of the catalyst. Figure 3 shows the product distribution of Hβ and Zn/Hβ catalysts in the ethanol conversion. Besides the target product of propylene, the main byproducts were CH_4, C_2H_4, C_4H_8, C_2-C_4 alkanes and C_{5+} (liquid phase products, aliphatic and aromatics) were also detected. Interestingly, Hβ gave a yield of ethylene up to 62.4 %, which is produced from the direct dehydration of ethanol. However, the yield of propylene was as low as 7.8%, which was expected to be produced via trimerization of ethylene followed by β-scission. In addition, Hβ zeolite gave a yield of C_4H_8 as low as 2.8%. There was a 21.1% yield of C_2-C_4 alkanes produced by olefin hydrogenation and/or hydrogen transfer reactions, of which the yields of C_2H_6, C_3H_8, and C_4H_{10} were 4.2%, 8.5%, and 8.4%, respectively. A small amount of the C_{5+} byproduct (5.6%) was produced via sequential steps through ethylene oligomerization, cracking and/or cyclization and hydrogen transfer reactions on acid sites of Hβ zeolite. The byproduct of methane could be negligible (less than 0.5%). When the Zn species were introduced into the Hβ zeolite through impregnation, a significant increase in the yield of propylene was observed. The yield of propylene followed the order of Zn/Hβ-C (43.4%) > Zn/Hβ-N (37.4%) > Zn/Hβ-Ac (29.2%) > Zn/Hβ-S (16.0%). However, the yield of ethylene was roundly lessen, followed by the order of Zn/Hβ-S (45.9%) > Zn/Hβ-N (34.1%) ≈ Zn/Hβ-Ac (33.6%) > Zn/Hβ-C (30.8%). It is quite probable that the trimerization of ethylene followed by β-scission was significantly enhanced on the Zn species, leading to a higher yield of propylene and a lower yield of ethylene. Moreover, the yield of C_2-C_4 alkanes (1.5~4.3%) was also significantly reduced, which is attributed to the fact that the olefin hydrogenation and/or hydrogen transfer reactions were suppressed by the Zn species of Zn/Hβ catalysts. There was a clear increase on the yield of C_{5+} byproduct, which was from 10.1% for Zn/Hβ-N to 28.8% for Zn/Hβ-S. Based on the above results, the type of zinc precursors has a significant effect on the catalytic reactivity of Zn/Hβ in the ethanol to propylene reaction.

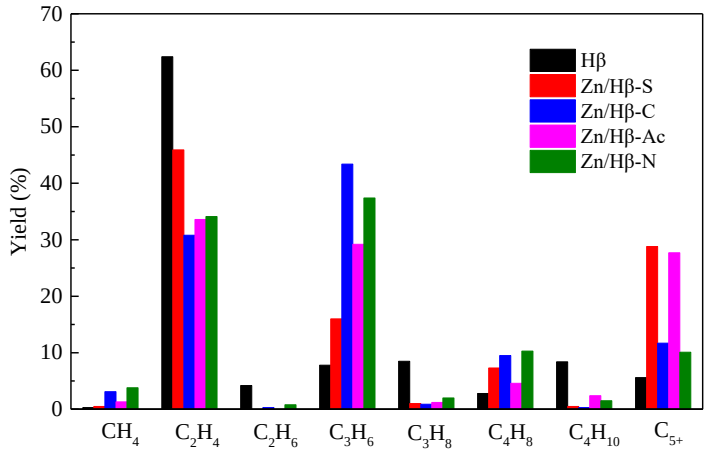

 doi:10.20944/preprints202403.1382.v1

Figure 3. Catalytic performance of Hβ and Zn/Hβ catalysts in the ethanol conversion. Reaction conditions: 500 °C, 0.1 MPa, P_{C2H5OH} = 0.02 MPa, *WHSV* = 2.8 h^{-1}, TOS = 1 h.

Figure 4 shows the evolution of propylene yield with TOS of 7 h over Hβ and Zn/Hβ catalysts in the ethanol conversion. The ethanol conversion always remained 100% for all of the catalysts during the reaction. For the propylene product, the propylene yield of Hβ at TOS = 0.68 h was only 9.3%, and gradually declined to 2.0% after TOS of 7 h. In contrast, Zn/Hβ gave a higher propylene yield than that of Hβ at the same reaction time. The propylene yield at TOS = 0.68 h followed the sequence of Zn/Hβ-C (44.9%) > Zn/Hβ-S (38.9%) ≈ Zn/Hβ-Ac (38.7%) > Zn/Hβ-N (28.2%). The propylene yield over Zn/Hβ-S, Zn/Hβ-C and Zn/Hβ-Ac was gradually declined with prolonging TOS, while the propylene yield of Zn/Hβ-N was first increased to 35.4% at TOS = 1 h and then decreased to 13.5% at the end of the reaction. Among these Zn/Hβ catalysts, the lowest decline of the propylene yield was observed for Zn/Hβ-S, and the relatively high propylene yield of 19.0% was still achieved after TOS of 7 h. It is concluded that Zn/Hβ-S exhibited better stability than other catalysts in the ethanol conversion.

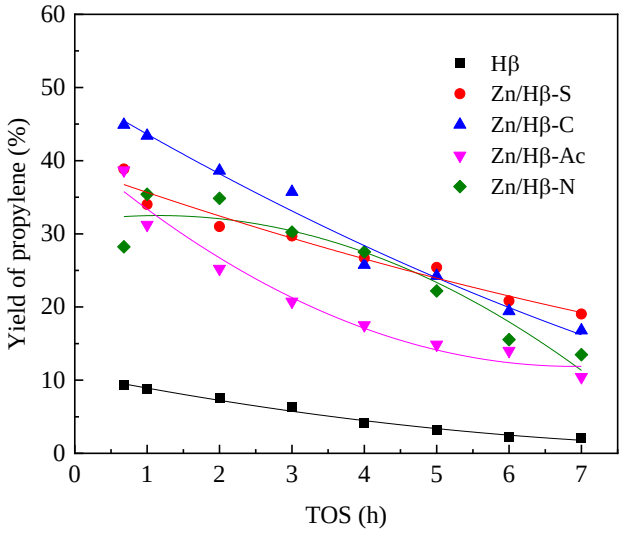

Figure 4. Evolution of propylene yield with TOS over Hβ and Zn/Hβ catalysts in the ethanol conversion. Reaction conditions: 500 °C, 0.1 MPa, P_{C2H5OH} = 0.02 MPa, *WHSV* = 2.8 h^{-1}.

3.4. Deactivation of the catalysts

It is widely accepted that the coke deposition is one of the main reasons for the deactivation of the zeolite-based catalyst in the ethanol conversion. In this respect, TPO experiments were firstly conducted to determine the coke species on the used catalysts after TOS of 7 h. The resultant TPO profiles of the used Hβ and Zn/Hβ catalysts are shown in Figure 5. Clearly, a broad oxygen consumption peak in the temperature region of 350 to 750 °C was observed for all of the catalysts, indicating the presence of the varied type of coke species. Generally, the peak temperature of oxygen consumption is used to be an common indicator for identifying the type of coke species, which the peak temperature of the heavy coke species is higher. Meanwhile, to semi-quantitatively determine the amount of coke species, the TPO profiles were deconvoluted into two peaks based on the peak temperature of oxygen consumption. The first peak (Peak I) at around 510-550 °C was attributed to the light coke corresponding to hydrogenated species, while the second peak at around 580-640 °C was assigned to the heavy coke corresponding to carbonaceous species [32]. Thus, the peak temperature (T_{max}) and the corresponding peak area of oxygen consumption are summarized in Table 3.

 doi:10.20944/preprints202403.1382.v1

As shown in Figure 5 and Table 3, it is found that the total oxygen consumption of the used catalysts followed the order of Zn/Hβ-S > Hβ > Zn/Hβ-C > Zn/Hβ-Ac > Zn/Hβ-N, indicating the same order of the total coke amount. Specifically, the peak area of the Peak I followed the order of Zn/Hβ-S > Zn/Hβ-C > Zn/Hβ-AC > Hβ > Zn/Hβ-N, while the peak area of the Peak II presented the order of Hβ > Zn/Hβ-S > Zn/Hβ-N > Zn/Hβ-AC > Zn/Hβ-C. Moreover, in the case of Zn/Hβ-C, Zn/Hβ-AC and Hβ, similar peak temperature of the Peak I at around 550 °C was achieved, higher than those of Zn/Hβ-S and Zn/Hβ-N, indicating the presence of the heavier coke species. However, the different order occurred on the peak temperature of the Peak II. For Hβ, Zn/Hβ-C and Zn/Hβ-AC, similar peak temperature of the Peak II at around 600-610 °C was observed, which is lower than that of Zn/Hβ-S (633 °C) and higher than that of Zn/Hβ-N (580 °C).

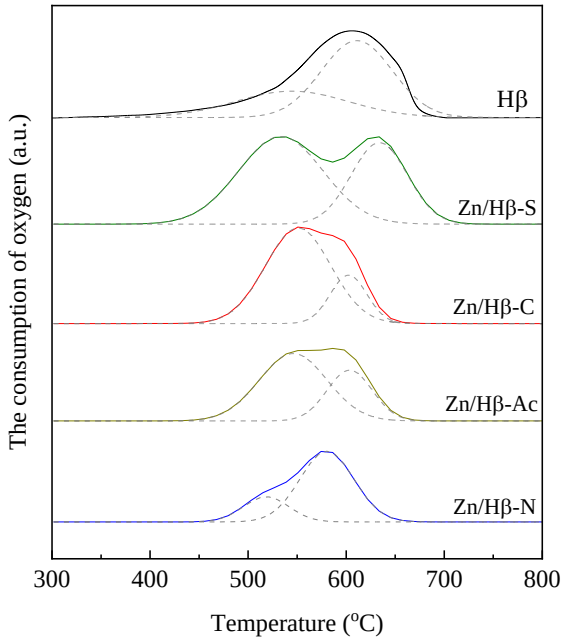

Figure 5. TPO profiles of used Hβ and Zn/Hβ catalysts.

Table 3. TPO results of used Hβ and Zn/Hβ catalysts.

Used catalyst	T_{max} (°C)		The consumption of oxygen (a.u./g)		
	Peak I	Peak II	Peak I	Peak II	Total
Hβ	545	611	25.8	47.5	73.3
Zn/Hβ-S	533	634	64.2	39.7	103.9
Zn/Hβ-C	551	602	54.1	15.4	69.5
Zn/Hβ-Ac	546	603	39.6	19.8	59.4
Zn/Hβ-N	518	580	9.9	33.1	43.0

The FTIR characterization was used to further investigate coke deposited on these catalysts during the ethanol conversion. Figure 6 shows the FTIR spectra of both fresh and used catalysts in the framework vibration region of 1300-1800 and 2800-3000 cm^{-1}. All of the catalysts contained adsorbed water which was observed at the band of 1637 cm^{-1} [33]. Compared with the fresh catalysts, there were new bands observed on used catalysts. The bands at 1355 and 1456 cm^{-1} are attributed to

 doi:10.20944/preprints202403.1382.v1

the CH_3 bending vibrations of aliphatics. The band at 1590 cm^{-1} corresponds to polyaromatic hydrocarbons and condensed coke. The bands in 1618 cm^{-1} is due to dienes and C=C double bonds in carbon chains. The bands located at 2852 and 2870 cm^{-1} are assigned to the symmetric vibrations of CH_2 and CH_3 groups, respectively, while the bands at 2925 and 2958 cm^{-1} are due to the asymmetric vibrations of the same groups [33–35].

Hβ zeolite showed a higher intensity of the band at 1590 cm^{-1}, indicating the presence of a higher proportion of aromatic coke. It could be because the wide channels of Hβ are beneficial for oligomerization, cyclization, aromatization, etc. and resulted in the generation of macromolecular compounds such as polyaromatics. L. Pinard et al. [34] identified the coke species of Hβ in the ethanol conversion were alkybenzenes, mainly hexamethylbenzenes and alkyl-pyrenes, which is found to be the main compounds in the pores. Compared with Hβ, Zn/Hβ catalysts exhibited higher intensity of the bands at 1618 cm^{-1}, indicating that the higher proportion of olefinic coke. It could be because the channels of Hβ tend to be narrow after impregnation, giving rise to inhibit polyaromatics formation during the reaction. Furthermore, both 1590 and 1618 cm^{-1} bands were higher for used Zn/Hβ-S than other used catalysts, indicating the presence of more olefinic and aromatic coke. This is mainly attributed to the highest amount of strong acid sites on Zn/Hβ-S. It can be reasonably explained that the ethene oligomerization, cyclization, aromatization, condensation, and hydrogen transfer reaction would occur preferentially on strong acid sites.

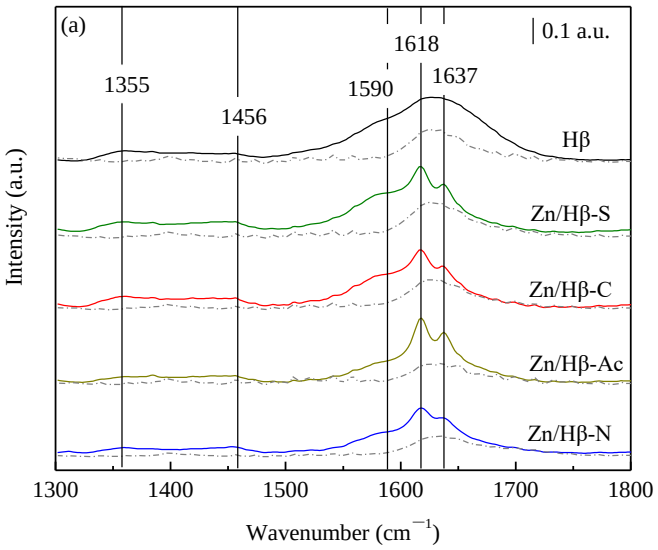

 doi:10.20944/preprints202403.1382.v1

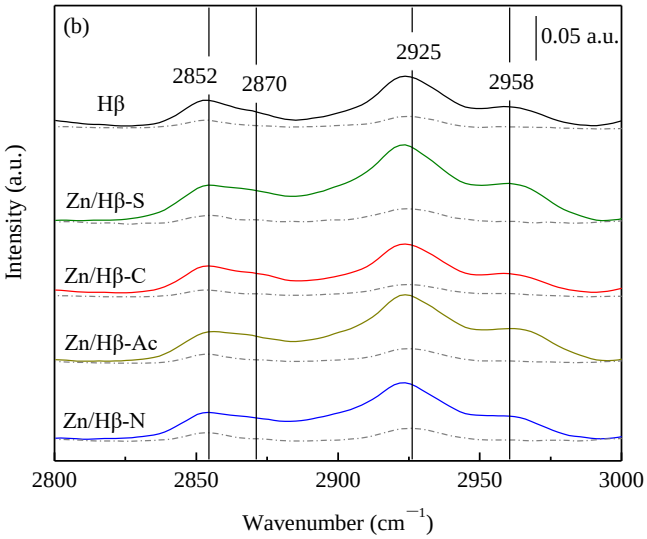

Figure 6. FTIR spectra of both fresh (dash dot line) and used (solid line) Hβ and Zn/Hβ catalysts in the region of 1300-1800 (a) and 2800-3000 cm^{-1} (b).

4. Discussion

4.1. Key factors effecting the catalytic activity

As is well known, the catalytic performance of the zeolite in the conversion of ethanol to propylene is closely related to the amount and strength distribution of acid site [13,22]. The reaction pathway is generally accepted to be that ethanol is firstly dehydrated to produce ethylene, followed by the oligomerization-cracking way to produce propylene [10–12]. Taking the randomness of the oligomerization into account, the propylene yield is below 20-30%, and the main byproduct are ethylene, butenes, C_2-C_4 alkanes and C_{5+} including liquid phase products, aliphatic and aromatics, etc. Expectedly, Hβ gave a yield of ethylene up to 62.4 % and a yield of propylene as low as 7.8% in this work. Simultaneously, a considerable amount of C_2-C_4 alkanes up to 21.1% was yielded by olefin hydrogenation and/or hydrogen transfer reactions (Figure 3). These results are consistent with the catalytic activity of HBeta zeolite reported in the literature [22].

Based on the above NH_3-TPD results, the acidity of Zn/Hβ catalysts can be easily tuned by employing the different zinc precursors (Figure 2 and Table 2). As a result, the catalytic performance was significantly affected in the conversion of ethanol to propylene. To reveal the effect of acidity on the catalytic performance of Zn/Hβ, the correlation analysis was carried out between both the amount of acid sites and S/(W+M) ratio and the propylene yield, and the results are shown in Figure 8. The S/(W+M) ratio represents the ratio of strong acid sites to the sum of weak and medium acid sites. However, after carefully comparative analysis, there is no regular variation pattern between the acidity and the propylene yield, which is used to be the most important index of catalytic activity. This may be strongly related to the uneven distribution of acidity on surface of the Zn/Hβ catalysts. On the other hand, the reaction pathway for Zn/Hβ catalysts may be different from Hβ according to the previous works. Miao et al. [22] reported that a high yield of propylene up to 50% was achieved for the In_2O_3-beta composites by promoting the intermediate of acetone to propylene instead of the byproduct isobutene, when the proposed reaction pathway could be ethanol → acetaldehyde → acetone → isopropanol → propylene. Similarly, Zhang et al. [23] proposed the reaction pathway over the $ZnCeO_x$ and HBeta composites could be ethanol → acetaldehyde → ethyl acetate → acetone → isopropanol → propylene. Moreover, it is found that the basicity of $ZnCeO_x$ plays an vital role for the ethanol dehydrogenation to acetaldehyde, but the acidity of catalysts is more important for the propylene selectivity. Hence, these proposed reaction pathways over the metal oxides and HBeta

 doi:10.20944/preprints202403.1382.v1

composites are completely different from the Hβ, where the ethanol directly dehydrates to ethylene followed by the oligomerization-cracking way to produce propylene. For this reason, it is reasonable to refer that a very similar reaction pathway of ethanol to propylene can be proposed for the Zn/Hβ catalysts.

Based on the above analysis, it can be concluded that the moderate amount of acid sites and S/(W+M) ratio on Zn/Hβ were more beneficial to the formation of propylene in the ethanol conversion. The Zn/Hβ catalysts can not only promote the propylene yield from an additional reaction pathway of ethanol → acetaldehyde → acetone → isopropanol→ propylene, but also suppress the secondary reactions of propylene and the side reactions of key intermediate. As a result, Zn/Hβ-C exhibited the highest propylene yield of 43.4% at TOS = 1.0 h.

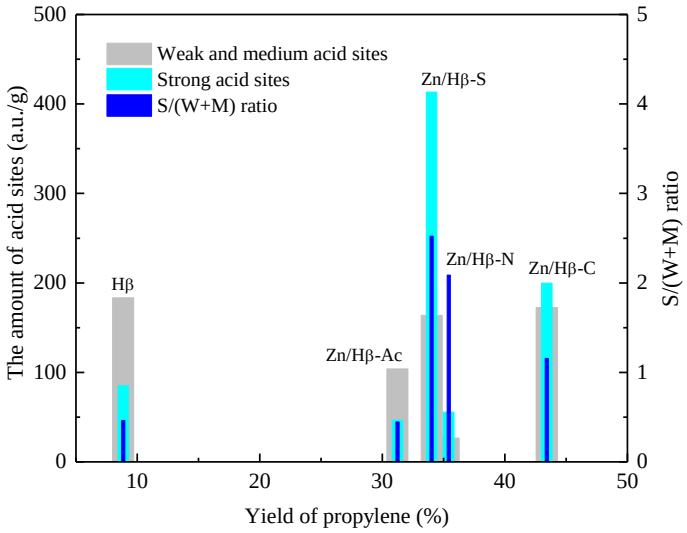

Figure 7. Corrections between acidic properties and propylene yield in the ethanol conversion over Zn/Hβ catalysts with different zinc precursors. Reaction conditions: 500 °C, 0.1 MPa, P_{C2H5OH} = 0.02 MPa, *WHSV* = 2.8 h^{-1}, TOS=1 h.

4.2. Deactivation mechanism

The conversion of ethanol to propylene is usually accompanied by a number of side reactions that result in the formation of coke deposition. It is well known that the coke originates from the condensation of intermediates that are also activated by the acid sites. To further understand the effect of acidity on the coking behaviors of the used Zn/Hβ catalysts, the amounts of different acid sites with average coking rate (ACR) are correlated in Figure 8. The average coking rate (a.u./(g·h)) is identified as the consumption of oxygen per gram used catalyst in an hour. From Figure 8, it is observed that the average coking rate of used Zn/Hβ was strongly related to the amount of total acid sites, especially the strong acid sites. To be specific, the higher the amount of total acid sites of the catalyst, the greater average coking rate. These results indicate that the strong acid sites were mainly responsible for coke deposition in the ethanol conversion to propylene, which is consistent with the results reported in the literature [23]. In addition, the coke composition is also affected by the strength distribution of acid sites. The FT-IR results showed that a high proportion of aromatic coke was deposited on the used Zn/Hβ-S, which exhibited the relatively high amount of strong acid sites. The reactions including oligomerization, trimerization, cyclization, aromatization would occurred steadily on the strong acid sites. As is well known, aromatic coke is difficult to remove, giving rise to the catalyst deactivation. However, every coin has two sides. The precursors of aromatic coke were commonly used as active groups and/or the intermediates in the reaction. Madeira et al. found that the active groups included dehydrogenated species such as alkylated aromatics [5]. Thus, for the

 doi:10.20944/preprints202403.1382.v1

catalyst with a larger amount of coke deposition after TOS of 7 h, it can be reasonably explained that a higher propylene yield as high as 19.0% was still retained for Zn/Hβ-S.

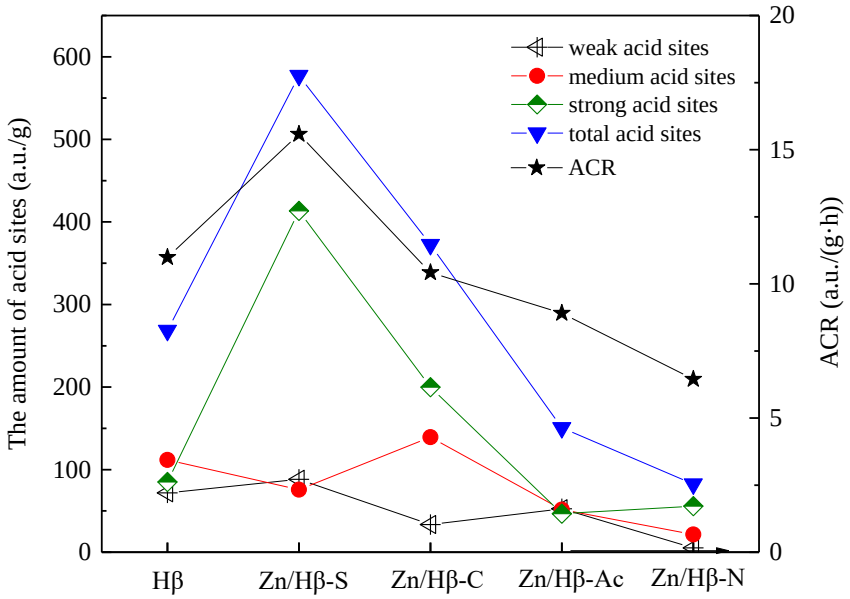

Figure 8. Corrections between acidic properties and the average coking rate of used Zn/Hβ catalysts in the ethanol conversion.

5. Conclusion

In summary, the amount and strength distribution of acid sites on Zn/Hβ catalysts were simply tuned by introducing the different type of zinc precursors, and further affected the propylene yield in ethanol conversion. Specifically, when the Zn species were introduced to the Hβ, the propylene yield was significantly enhanced, whereas the yields of the byproducts such as ethylene and C_2-C_4 alkane were remarkably suppressed. In the case of the catalyst prepared by using the $ZnCl_2$ precursor, Zn/Hβ-C showed a higher propylene up to 43.3%, which is due to the moderate amount and strength distribution of acid sites. Both the total coke amount and the average coking rate of the used Zn/Hβ catalysts were closely associated with the amount of total acid sites, especially the strong acid sites. The higher the amount of total acid sites of the catalyst, the greater the total coke amount and average coking rate. For the catalyst with a larger amount of coke deposition after TOS of 7 h, a higher propylene yield as high as 19.0% was still preserved for Zn/Hβ-S prepared by using the $ZnSO_4{\cdot}7H_2O$ precursor, which is attributed to the higher amount of strong acid sites.

Acknowledgments: The financial supports from the Natural Science Basic Research Plan in Shaanxi Province of China (2022JQ-085) and Special Research Projects of Shaanxi Province of China (19JK0673) are highly appreciated.

Declaration of Competing Interests: There are no conflicts to declare.

References

1. Matheus CRV, Aguiar EFS. The role of MPV reaction in the synthesis of propene from ethanol through the acetone route. Catalysis Communications. 2020; 145: 106096.
2. R. V. Matheus C, H. Chagas L, G. Gonzalez G, Falabella S. Aguiar E, G. Appel L. Synthesis of Propene from Ethanol: A Mechanistic Study. ACS Catalysis. 2018; 8: 7667-7678.
3. Licht RB, Bell AT. A DFT Investigation of the Mechanism of Propene Ammoxidation over α-Bismuth Molybdate. ACS Catalysis. 2016; 7: 161-176.
4. Hussain AI, Aitani AM, Kubů M, Čejka J, Al-Khattaf S. Catalytic cracking of Arabian Light VGO over novel

 doi:10.20944/preprints202403.1382.v1

zeolites as FCC catalyst additives for maximizing propylene yield. Fuel. 2016; 167: 226-239.
5. Phung TK, Pham TLM, Vu KB, Busca G. (Bio)Propylene production processes: A critical review. Journal of Environmental Chemical Engineering. 2021; 9: 105673.
6. Song S, Sun Y, Yang K, Fo Y, Ji X, Su H, Li Z, Xu C, Huang G, Liu J, Song W. Recent Progress in Metal-Molecular Sieve Catalysts for Propane Dehydrogenation. ACS Catalysis. 2023; 13: 6044-6067.
7. Sun J, Wang Y. Recent Advances in Catalytic Conversion of Ethanol to Chemicals. ACS Catalysis. 2014; 4: 1078-1090.
8. Yin J, Guo X, Sun Y, Han S, Li Q. Understanding the Nanoconfinement Effect on the Ethanol-to-Propene Mechanism Catalyzed by Acidic ZSM-5 and FAU Zeolites. The Journal of Physical Chemistry C. 2021; 125: 310-334.
9. Huangfu J, Mao D, Zhai X, Guo Q. Remarkably enhanced stability of HZSM-5 zeolite co-modified with alkaline and phosphorous for the selective conversion of bio-ethanol to propylene. Applied Catalysis A: General. 2016; 520: 99-104.
10. Duan C, Zhang X, Zhou R, Hua Y, Zhang L, Chen J. Comparative studies of ethanol to propylene over HZSM-5/SAPO-34 catalysts prepared by hydrothermal synthesis and physical mixture. Fuel Processing Technology. 2013; 108: 31-40.
11. Xia W, Chen K, Takahashi A, Li X, Mu X, Han C, Liu L, Nakamura I, Fujitani T. Effects of particle size on catalytic conversion of ethanol to propylene over H-ZSM-5 catalysts—Smaller is better. Catalysis Communications. 2016; 73: 27-33.
12. Xia W, Takahashi A, Nakamura I, Shimada H, Fujitani T. Study of active sites on the MFI zeolite catalysts for the transformation of ethanol into propylene. Journal of Molecular Catalysis A: Chemical. 2010; 328: 114-118.
13. Li X, Kant A, He Y, Thakkar HV, Atanga MA, Rezaei F, Ludlow DK, Rownaghi AA. Light olefins from renewable resources: Selective catalytic dehydration of bioethanol to propylene over zeolite and transition metal oxide catalysts. Catalysis Today. 2016; 276: 62-77.
14. Xia W, Wang J, Wang L, Qian C, Ma C, Huang Y, Fan Y, Hou M, Chen K. Ethylene and propylene production from ethanol over Sr/ZSM-5 catalysts: A combined experimental and computational study. Applied Catalysis B: Environmental. 2021; 294: 120242.
15. Zhang N, Mao D, Zhai X. Selective conversion of bio-ethanol to propene over nano-HZSM-5 zeolite: Remarkably enhanced catalytic performance by fluorine modification. Fuel Processing Technology. 2017; 167: 50-60.
16. Huang R, Fung V, Wu Z, Jiang D-e. Understanding the conversion of ethanol to propene on In2O3 from first principles. Catalysis Today. 2020; 350: 19-24.
17. Hayashi F, Iwamoto M. Yttrium-Modified Ceria As a Highly Durable Catalyst for the Selective Conversion of Ethanol to Propene and Ethene. ACS Catalysis. 2012; 3: 14-17.
18. Hayashi F, Tanaka M, Lin D, Iwamoto M. Surface structure of yttrium-modified ceria catalysts and reaction pathways from ethanol to propene. Journal of Catalysis. 2014; 316: 112-120.
19. Wang F, Xia W, Mu X, Chen K, Si H, Li Z. A combined experimental and theoretical study on ethanol conversion to propylene over Y/ZrO2 catalyst. Applied Surface Science. 2018; 439: 405-412.
20. Xia W, Wang F, Mu X, Chen K. Remarkably enhanced selectivity for conversion of ethanol to propylene over ZrO2 catalysts. Fuel Processing Technology. 2017; 166: 140-145.
21. Iwamoto M, Tanaka M, Hirakawa S, Mizuno S, Kurosawa M. Pulse and IR Study on the Reaction Pathways for the Conversion of Ethanol to Propene over Scandium-Loaded Indium Oxide Catalysts. ACS Catalysis. 2014; 4: 3463-3469.
22. Xue F, Miao C, Yue Y, Hua W, Gao Z. Direct conversion of bio-ethanol to propylene in high yield over the composite of In2O3 and zeolite beta. Green Chem. 2017; 19: 5582-5590.
23. Xu L, Zhao R, Zhang W. One-step high-yield production of renewable propene from bioethanol over composite ZnCeOx oxide and HBeta zeolite with balanced Brönsted/Lewis acidity. Applied Catalysis B: Environmental. 2020; 279: 119389.
24. Jin H, Yue Y, Miao C, Tian C, Hua W, Gao Z. Direct and Highly Selective Conversion of Bioethanol to Propylene Over Y-CeO2 and Zeolite Beta Composite. Catal Lett. 2022; 153: 230-238.
25. Xue F, Miao C, Yue Y, Hua W, Gao Z. Sc2O3-promoted composite of In2O3 and Beta zeolite for direct conversion of bio-ethanol to propylene. Fuel Processing Technology. 2019; 186: 110-115.
26. Islam MJ, Granollers Mesa M, Osatiashtiani A, Taylor MJ, Manayil JC, Parlett CMA, Isaacs MA, Kyriakou G. The effect of metal precursor on copper phase dispersion and nanoparticle formation for the catalytic transformations of furfural. Applied Catalysis B: Environmental. 2020; 273: 119062.
27. Shao B, Ren K, Zhang C, Lin M, Zhou S, Li Y, Zong B. Effect of Metal Precursors on the Performance of Pt/Y Catalysts for Isobutane-Butene Alkylation Reaction-Regeneration. Industrial & Engineering Chemistry

Research. 2023; 62: 19619-19628.
28. Zhang B, Zhu X, Gao J, Zhu Y, Ma W. Zn modification of Beta zeolite: Effect on acid sites and propylene oxide rearrangement. Chemical Physics. 2020; 539: 110983.
29. Rehman AU, Khan M, Maosheng Z. Hydration behavior of MgSO4–ZnSO4 composites for long-term thermochemical heat storage application. Journal of Energy Storage. 2019; 26: 101026.
30. Kurban GVT, Rego ASC, Mello NM, Brocchi EA, Navarro RCS, Souza RFM. Thermodynamics and Kinetic Modeling of the ZnSO4·H2O Thermal Decomposition in the Presence of a Pd/Al2O3 Catalyst. Energies. 2022; 15: 548.
31. Liao W, Tang C, Zheng H, Ding J, Zhang K, Wang H, Lu J, Huang W, Zhang Z. Tuning activity and selectivity of CO2 hydrogenation via metal-oxide interfaces over ZnO-supported metal catalysts. Journal of Catalysis. 2022; 407: 126-140.
32. Bai T, Zhang X, Wang F, Qu W, Liu X, Duan C. Coking behaviors and kinetics on HZSM-5/SAPO-34 catalysts for conversion of ethanol to propylene. J Energy Chem. 2016; 25: 545-552.
33. Sousa ZSB, Cesar DV, Henriques CA, Teixeira da Silva V. Bioethanol conversion into hydrocarbons on HZSM-5 and HMCM-22 zeolites: Use of in situ DRIFTS to elucidate the role of the acidity and of the pore structure over the coke formation and product distribution. Catalysis Today. 2014; 234: 182-191.
34. Pinard L, Tayeb KB, Hamieh S, Vezin H, Canaff C, Maury S, Delpoux O, Pouilloux Y. On the involvement of radical “coke” in ethanol conversion to hydrocarbons over HZSM-5 zeolite. Catalysis Today. 2013; 218-219: 57-64.
35. Ferreira Madeira F, Ben Tayeb K, Pinard L, Vezin H, Maury S, Cadran N. Ethanol transformation into hydrocarbons on ZSM-5 zeolites: Influence of Si/Al ratio on catalytic performances and deactivation rate. Study of the radical species role. Applied Catalysis A: General. 2012; 443-444: 171-180.